IOP Conference Series: Materials Science and Engineering

Effect of non-linear thermal radiation on MHD Siko nanofluid flow over a bidirectional stretching surface

To cite this article: M Sathish Kumar *et al* 2017 *IOP Conf. Ser.: Mater. Sci. Eng.* **263** 062023

IOP Conf. Series: Materials Science and Engineering **263** (2017) 062023 doi:10.1088/1757-899X/263/6/062023

Effect of non-linear thermal radiation on MHD Siko nanofluid flow over a bidirectional stretching surface

M Sathish Kumar[1], N, Sandeep[1], B Rushi Kumar[1] and R Vijayaragavan[2]
[1]Department of Mathematics, School of Advanced Sciences, VIT University, Vellore-632014, India
[2]Department of Mathematics, Thiruvalluvar University, Vellore-632115, India

E-mail: dr.nsrh@gmail.com

Abstract. The three-dimensional magnetohydrodynamic flow and heat transfer of Sisko nanofluid across a bidirectional stretching sheet are examined numerically. Nonlinear thermal radiation is incorporated into the energy equation. The reduced governing PDEs are solved by using the bvp5c Matlab package. The local Nusselt number and wall friction are computed at different pertinent parameters. With the help of graphical illustrations, we studied the momentum and thermal boundary layer behavior. It is found that the flow and thermal boundary layers of Cu-water nanofluid are higher than the methanol-Cu nanofluid.

1. Introduction

The MHD heat transfer of Sisko nanofluid past stretching surface has significant applications in mechanical and engineering fields. Such flows normally involve in wire drawing, hot rolling, production of glass fiber, plastic sheets extrusion, and paper production, etc. The Sisko fluid is one of the non-Newtonian fluids. The most suitable example of Sisko nanofluid is lubricating greases [1]. The flow induced in constantly moving plate [2]. The 3D flow owing to a stretching surface [3]. The impact of viscous dissipation on heat transfer stream towards a stretching surface by considering heat generation [4].

In recent times, many researchers are analyzing Sisko nanofluid model with different various geometries and different physical assumptions. The study of the 2D MHD flow of micropolar fluid towards a stretching sheet with magnetic field [5]. The influence of variable viscosity lying on unsteady MHD heat transfer flow past a stretching sheet with variable fluid properties[6]. Heat transfer flow of non-Newtonian fluid towards a stretching surface with cross diffusion effect and concluded that the rising value of thermophoresis parameter encourages the Nusselt number [7]. The impact of viscous dissipation and chemical reaction on MHD convection flow towards a stretching surface with magnetic field[8]. The steady 2D heat transfer flow of non-Newtonian fluid towards a stretching surface [9]. Numerical investigation of non-Newtonian fluid towards a stretching cylinder by an account of thermal conductivity[10]. MHD mass transfer flow Casson fluid over a wedge in the presence of nonlinear radiation and solved numerically by R-K and Newton technique [11].

The numerical investigation of magnetohydrodynamic flow of non-Newtonian fluid past a stretching tube by considering thermal conductivity[12]. The MHD axisymmetric Sisko fluid flows past a stretching surface and solved numerically by shooting method [13]. Effect of slanting magnetic field of non-Newtonian fluid over a stretching surface [14] and concludes that rising value of magnetic field parameter boosted the reduced Nusselt number. The impact of viscous dissipation and radiation on mixed convection flow of non- Newtonian fluid past a stretching sheet [15]. The unsteady 2D non-Newtonian fluids past a stretching sheet [16]. The heat transfer of MHD Cu-water flow past a wedge and cone with viscous dissipation [17]. Unsteady 2D MHD Carreau fluid flow over stretching surface with cross diffusion effect [18]. The numerical investigation of MHD non-Newtonian fluid flow towards a stretching sheet with non-linear thermal radiation [19] and numerically solved by using R-K with shooting technique. The influence of thermal radiation effect on MHD heat transfer flow past a vertical plate [20].

Motivated by the above studies, in this paper, we investigated the 3D magnetohydrodynamic momentum and heat transfer of Sisko nanofluid across a bidirectional stretching surface is examined numerically. Nonlinear thermal radiation is included in the heat equation. The reduced governing PDEs are solved by using the bvp5c Matlab package. The reduced Nusselt number and wall friction are computed at different pertinent parameters. With the help of graphical illustrations, we studied the velocity and thermal boundary layer behavior.

2. Mathematical formulation

Consider a steady 3D, magneto hydrodynamic flow of a Sisko nanofluid towards a bi-directional stretching sheet with nonlinear thermal radiation. The sheet coexists with the flat surface $z=0$ and the flow takes place in the domain $z>0$.The constant surface is being extended with the linear velocities dy and cx in the y and x directions, correspondingly. The d and c constants are certain genuine numbers identifying with the stretching surface. Heat transfer analysis is taken into an account with nonlinear thermal radiation effect. The ambient fluid temperature is taken T_∞. (See Figure.1)

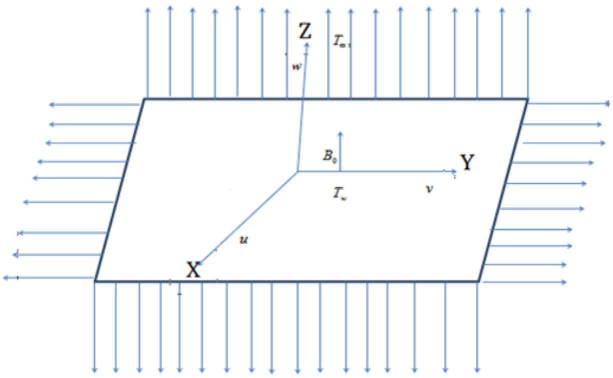

Figure. 1 Physical geometry

The governing equations of the 3D heat transfer of Sisko nanofluid are expressed under boundary layer assumptions are as follows:

$$\frac{\partial u}{\partial x}+\frac{\partial v}{\partial y}+\frac{\partial w}{\partial z}=0, \tag{1}$$

$$\rho_{nf}\left(u\frac{\partial u}{\partial x}+v\frac{\partial u}{\partial y}+w\frac{\partial u}{\partial z}\right)=a\frac{\partial^2 u}{\partial z^2}-b\frac{\partial}{\partial z}\left[\left(\frac{\partial u}{\partial z}\right)^n\right]-\sigma B_0^2 u, \tag{2}$$

$$\rho_{nf}\left(u\frac{\partial v}{\partial x}+v\frac{\partial v}{\partial y}+w\frac{\partial v}{\partial z}\right)=a\frac{\partial^2 v}{\partial z^2}+b\frac{\partial}{\partial z}\left[\left(-\frac{\partial u}{\partial z}\right)^{n-1}\right]\frac{\partial v}{\partial z}-\sigma B_0^2 v, \tag{3}$$

$$u\frac{\partial T}{\partial x}+v\frac{\partial T}{\partial y}+w\frac{\partial T}{\partial z}=\frac{k_{nf}}{(\rho c_p)_{nf}}\frac{\partial^2 T}{\partial z^2}+\frac{16\sigma^*}{3k^*(\rho c_p)_{nf}}\frac{\partial T}{\partial z}\left(T^3\frac{\partial T}{\partial z}\right), \tag{4}$$

where (u,v,w) - velocity components along with x, y and z directions respectively, ρ_{nf} - nanofluid density, T -temperature, σ - electrical conductivity, $(\rho c_p)_{nf}$ -heat capacity of nanofluid B_0 - applied magnetic field strength and k_{nf} - thermal conductivity. The constants nano fluids are as follows:

$$(\rho c_p)_{nf}=(1-\phi)(\rho c_p)_f+\phi(\rho c_p)_s\,,\ \mu_{nf}=\frac{\mu_f}{(1-\phi)^{2.5}}$$

$$\frac{k_{nf}}{k_f}=\frac{(k_s+2k_f)-2\phi(k_f-k_s)}{(k_s+2k_f)+\phi(k_f-k_s)},\ \rho_{nf}=(1-\phi)\rho_f+\phi\rho_s, \tag{5}$$

where ϕ - nano particle volume fraction. Subscripts s and f denotes solid and fluid friction properties respectively.

The corresponding conditions are

$$v=v_w(y)=dy, u=u_w(x)=cx,\ \ w=0.\ T=T_\infty\ at\ z=0,$$
$$v\to 0, \mathrm{u}\to 0, w\to 0, T\to T_\infty\ as\ z\to\infty, \tag{6}$$

We now initiated the nondimensionalization system Eqs. 1-4 are as follows

$$v=cyg'(\eta),\ u=cxf'(\eta),\ w=-c\left(\frac{c^{n-2}}{\rho/b}\right)^{1/n+1}\left(\frac{2n}{n+1}f+\frac{1-n}{1+n}nf'+g\right)x^{(n-1)/(n+1)},$$

$$\theta(\eta)=\frac{T-T_\infty}{T_w-T_\infty},\ \eta=z\left(\frac{c^{2-n}}{b/\rho}\right)^{1/n+1}x^{(1-n)/(1+n)} \tag{7}$$

Subs. Eq.(7) in Eqs. (1) - (4), we find the following ODE equations:

$$\frac{A}{(1-\phi)^{2.5}}f'''+\left(1-\phi+\phi\left(\frac{\rho_s}{\rho_f}\right)\right)\left(\frac{2n}{n+1}ff''-(f')^2+gf''\right)-Mf'+n(-f'')^{n-1}f'''=0, \tag{8}$$

$$\frac{A}{(1-\phi)^{2.5}}g'''+\left(1-\phi+\phi\left(\frac{\rho_s}{\rho_f}\right)\right)\left(\frac{2n}{n+1}fg''-(g')^2+gg''\right)-Mg'+(-f'')^{n-1}g'''-(n-1)g''f'''(-f'')^{n-2}=0, \tag{9}$$

$$\frac{k_{nf}}{k_f}\frac{1}{\left(1-\phi+\phi\left((\rho c_p)_s/(\rho c_p)_f\right)\right)}\theta''+\left[R\left(1+(\theta_w-1)\theta\right)^3+3R\left(1+(\theta_w-1)\theta\right)^2(\theta_w-1)\theta'^2\right]$$
$$+\Pr\left(\left(\frac{2n}{n+1}\right)f\theta'+g\theta'\right)=0, \tag{10}$$

and boundary conditions (6) become

$$f(0)=0, g(0)=0, f'(0)=1,\ g'(0)=\lambda,\ \theta(0)\ =1,$$
$$f'(\eta)\to 0,\ f'(\eta)\to 0 \text{ and } \theta(\eta)\to 0 \text{ as } \eta\to\infty, \tag{11}$$

where λ - stretching ratio parameter, $\Pr$ - Prandtl number, A - material parameter, R - thermal radiation parameter,. Further, $\mathrm{Re}_a, \mathrm{Re}_b$ - reduced Reynolds number, which are given by

$$\mathrm{Re}_a=\frac{\rho xU}{a},\ \mathrm{Re}_b=\frac{\rho_f x^n U^{2-n}}{b},\ A=\frac{\mathrm{Re}_b^{\frac{2}{n+1}}}{\mathrm{Re}_a},\ \Pr=\frac{xUR_b^{\frac{-2}{n+1}}}{k_f/(\rho c_p)_f}, M=\frac{\sigma B_0^{\,2}}{c\rho_f}, \mathrm{R}=\frac{16\sigma^* T_\infty^3}{3k_f k^*}, \tag{12}$$

For the sake engineering, friction factor and heat transfer rates are established as

$$\frac{1}{2}\mathrm{Re}_b^{\,1/(n+1)}C_{fx}=(1-\phi)^{-2.5}\left[Af''(0)-(-f''(0))^n\right], \tag{13}$$

$$\frac{1}{2}\mathrm{Re}_b^{\,1/(n+1)}C_{fy}=(1-\phi)^{-2.5}\frac{v_w}{u_w}\left[Ag''(0)+\left[-f''(0)\right]^{n-1}g''(0)\right], \tag{14}$$

3. Analysis of results

The system of nonlinear ODE's Eqs.(8) - (10), with the subjected boundary condition Eq. (11), are numerically solved by using the bvp5c technique. In this study, we considered the various pertinent parameters values as $\phi=0.2, A=.5, n=3, R=2, \theta_w=1.1, \lambda=0.5, Le=1.$ These values are treated as constant throughout the study, excluding the variations in the relevant tables and figures. The impact of various non-dimensional parameters, namely magnetic field parameter, material parameter, nano particle volume fraction parameter, radiation parameter, and temperature ratio parameter on velocity and thermal fields are discussed with the help of graphs. Table 1 shows the thermo physical properties.

Figures. 2-4 are plotted to demonstrate the variations of $\theta(\eta)$, $f'(\eta)$ and $g'(\eta)$ for rising values of M . We have seen that the rising value of M enhances the $\theta(\eta)$ and opposite behavior is shown in

$g'(\eta)$ and $f'(\eta)$. Physically, increasing values of M produce the negative force in the flow direction, this force is known as drag force. This negative force helps to enhance the $\theta(\eta)$ and reduce the velocity fields. The effect of A on $\theta(\eta)$, $g'(\eta)$ and $f'(\eta)$ is shown in Figures. 5 - 7. It is evident that A helps to encourage $\theta(\eta)$ and depreciate both $g'(\eta)$ and $f'(\eta)$.

Figures. 8 - 10 shows that $\theta(\eta)$ increases and $g'(\eta), f'(\eta)$ decreases in rising values of ϕ.The velocity of the nanofluid is mutual to the particle size and growing the volume fraction enhances the thermal conductivity, due to this reason temperature profiles increases. Figure.11 exhibits $\theta(\eta)$ for various values of R. It is experimental that the rising values R encourage the $\theta(\eta)$. Generally, rising values of R release more heat energy to the flow, due to this reason rise in the temperature profiles for the rise in R is observed. The effect of θ_w on temperature profile is displayed in Figure. 12. It is evident that $\theta(\eta)$ has an increasing tendency with θ_w.This is due to rise in the thermal conductivity to the flow. Tables 2 and 3 shows the impact of the pertinent parameter on friction factor and reduced the Nusselt number. It is evident that the rising value of A, M and ϕ depreciate both wall friction and heat transfer rates. Increasing value of R and ϕ_w reduces the Nusselt number.

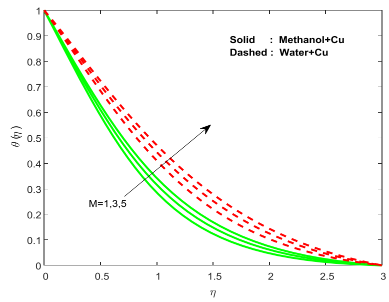

Figure 2. Effect of M on $\theta(\eta)$.

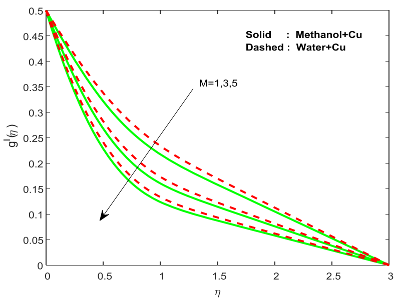

Figure 3. Effect of M on $g'(\eta)$.

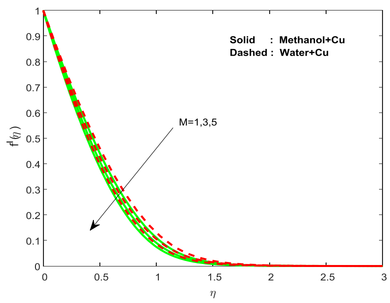

Figure 4. Effect of M on $f'(\eta)$.

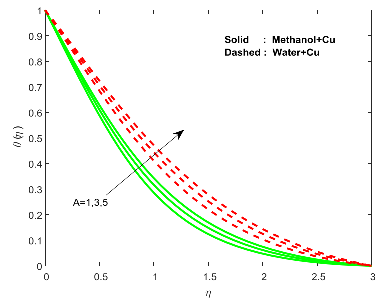

Figure 5. Effect of A on $\theta(\eta)$.

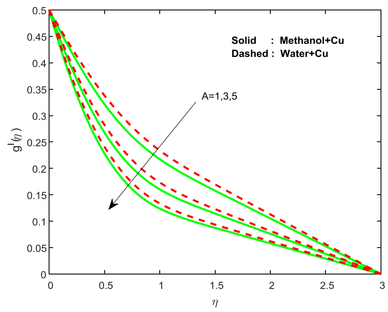

Figure 6. Effect of A on $g'(\eta)$.

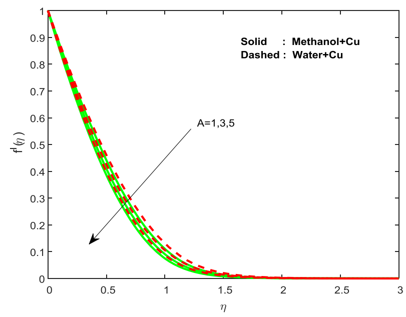

Figure 7. Effect of A on $f'(\eta)$.

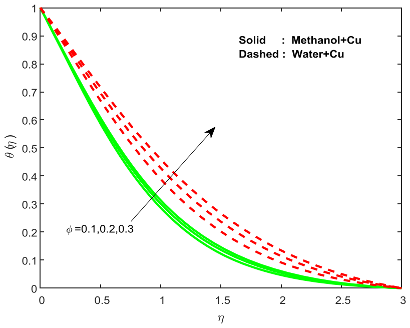

Figure 8. Effect of ϕ on $\theta(\eta)$.

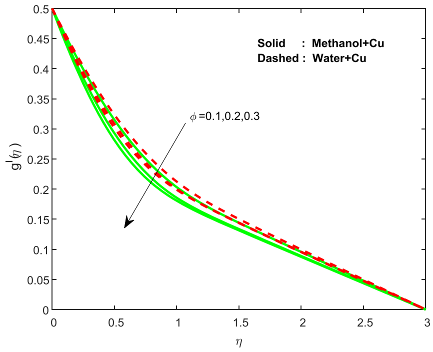

Figure 9. Effect of ϕ on $f'(\eta)$.

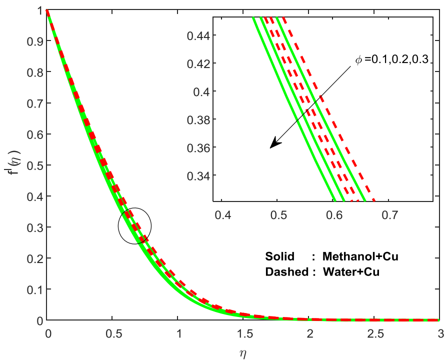

Figure 10. Effect of ϕ on $f'(\eta)$.

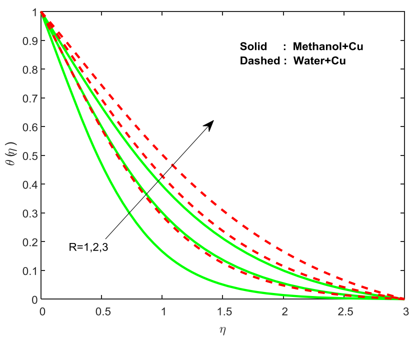

Figure 11. Effect of R on $\theta(\eta)$.

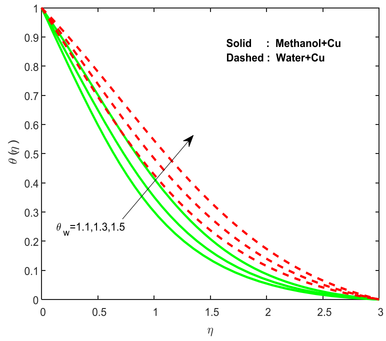

Figure 12. Effect of θ_w on $\theta(\eta)$.

Table 1 Thermo substantial properties of the methanol and water through base fluid

Physical properties	Methanol	Water	Copper
$\rho(\text{Kg/ m}^3)$	792	997	8933
$c_p(\text{J/ KgK})$	2545	4179	385
$k(\text{W/ mK})$	2035	0.613	400
Pr	7.38	6	--

Table 2. Friction factor and heat transfer coefficient of Sisko Nano fluid (Methanol+Cu) when $\phi = 0.2, A = .5, n = 3, R = 2, Le = 1, Kr = 0.5, \theta_w = 1.1, \lambda = 0.5$

M	A	ϕ	R	θ_w	$f''(0)$	$g''(0)$	$-\theta'(0)$
1					-1.305311	-0.412618	0.83137
3					-1.414214	-0.590548	0.78180
5					-1.505668	-0.746217	0.74085
	1				-1.305311	-0.412618	0.83137
	3				-1.414214	-0.590548	0.78180
	5				-1.505668	-0.746217	0.74085
		0.1			-1.287121	-0.436143	0.82446
		0.2			-1.362353	-0.504969	0.80539
		0.3			-1.408865	-0.550738	0.79176
			1		-1.362353	-0.504969	1.10971
			2		-1.362353	-0.504969	0.80539
			3		-1.362353	-0.504969	0.65244
				1.1	-1.362353	-0.504969	0.80539
				1.3	-1.362353	-0.504969	0.66451
				1.5	-1.362353	-0.504969	0.54054

Table 3. Friction factor and heat transfer coefficient of Sisko Nano fluid (Water+Cu) when $\phi = 0.2, A = .5, n = 3, R = 2, Le = 1, Kr = 0.5, \theta_w = 1.1, \lambda = 0.5$

M	A	ϕ	R	θ_w	$f''(0)$	$g''(0)$	$-\theta'(0)$
1					-1.255051	-0.369944	0.604162
3					-1.375127	-0.546696	0.557389
5					-1.473501	-0.702611	0.520168
	1				-1.255051	-0.369944	0.604162
	3				-1.375127	-0.546696	0.557389
	5				-1.473501	-0.702611	0.520168
		0.1			-1.260633	-0.413462	0.634297
		0.2			-1.318417	-0.461360	0.579441
		0.3			-1.351850	-0.489304	0.537745
			1		-1.318417	-0.461360	0.795542
			2		-1.318417	-0.461360	0.579441
			3		-1.318417	-0.461360	0.484946
				1.1	-1.318417	-0.461360	0.579441
				1.3	-1.318417	-0.461360	0.476950
				1.5	-1.318417	-0.461360	0.388188

4. Conclusions

The three-dimensional magnetohydrodynamic velocity and heat transfer of Sisko nanofluid across a bidirectional stretching surface is examined numerically. Nonlinear thermal radiation is incorporated into the energy equation. Findings of the present study are given by:

- Magnetic field parameter has a tendency to depreciate velocity profiles.
- Increasing value of A reducing the flow and Nusselt number.
- Rising values of temperature ratio parameter depreciate the local Nusselt number.

- Rising value of R increases the thermal boundary layer thickness.
- Rising values of volume fraction parameter encourage the heat energy of the fluid.

5. References

[1] Sisko A W 1958 *Industrial & Engineering Chemistry* **50** 1789-1792
[2] Sakiadis B C 1961 *AIChE J* **7** 221-225
[3] WangC Y 1984 *Physics of Fluids* 27 1915
[4] Vajravelu K and Hadjinicolaou A 1993 *Int. Com. in Heat and Mass Transfer* **20(3)** 417-430
[5] Hayat T, Abbas Z and Javed T 2008 *Physics Letters A* ***372*(5)** 637-647
[6] Mohmoud M A A and Megahed A M 2009 *Canadian J. of Phy*. **87(10)** 1065-1071
[7] Khan M, Malik R, Munir A and Khan W A 2015 *Plose One* **10(5)**
[8] Sandeep N and Sulochana C 2015 *Eng. Sci. and Tech., and Int. J.* **18(4)** 738-745
[9] Khan M and Shahzad A 2012 *Int. J. of Non-Linear Mech.* **47(9)** 999-1007
[10] Malik M Y, Hussain A, Salahuddin T and Awais M 2016 *J. of Mechanics* **32(5)** 593-601
[11] Raju C S K and Sandeep N 2017 *Acta Astronautica*
[12] Malik M Y, Hussain A, Salahuddin T, Awais A and Bilal S 2016 *AIP Advances* **6**
[13] Khan M, Malik R, Munir A and Shahzad A 2016 *J. of the Brazilian Soc. Of Mech. Sci. and Eng.* **38(4)** 1279-1289
[14] Malik A, Khan M, Munir A and Khan W A 2014 *Plos One* **9(10)**
[15] Khan M, Malik R and Munir A 2015 *AIP Advances* **5(8)**
[16] Raju C S K and Sandeep N 2016 *Alexandria Eng. J.* **55** 1115-1126
[17] Sandeep N and Gnaneswara Reddy M 2017 *J. of Molecular Liquids* **225** 87-94
[18] Khan M and Azam M 2017 *J. of Molecular Liquids* **225** 554-562
[19] Sathish Kumar M, Sandeep N, Rushi Kumar B and Prakash J 2017 *FHMT* **8** 8
[20] Raptis A 2017 *J. of Eng. Thermophysics* **26(1)** 53-59